Available online at www.sciencedirect.com
SCIENCE DIRECT®
Mendeleev Commun., 2007, **17**, 161–163
Mendeleev Communications

Redox properties and radical ions of 1,3λ⁴δ²,2,4-benzodithiadiazines in the hydrocarbon and fluorocarbon series

Nadezhda V. Vasilieva,[a] Irina G. Irtegova,[a] Nina P. Gritsan,*[b,c] Leonid A. Shundrin,[a] Anton V. Lonchakov,[b,c] Alexander Yu. Makarov,[a] Andrey V. Zibarev*[a,c]

[a] *N. N. Vorozhtsov Institute of Organic Chemistry, Siberian Branch of the Russian Academy of Sciences, 630090 Novosibirsk, Russian Federation. Fax: + 7 383 330 9752; e-mail: zibarev@nioch.nsc.ru*
[b] *Institute of Chemical Kinetics and Combustion, Siberian Branch of the Russian Academy of Sciences, 630090 Novosibirsk, Russian Federation. Fax: + 7 383 330 7350; e-mail: gritsan@kinetics.nsc.ru*
[c] *Department of Physics, Novosibirsk State University, 630090 Novosibirsk, Russian Federation*

DOI: 10.1016/j.mencom.2007.05.010

The first steps of electrochemical oxidation and reduction of the title compounds were studied by cyclic voltammetry, and electrochemically generated long-lived radical cations were characterised by ESR measurements and DFT calculations at the UB3LYP level of theory.

The redox properties of Group15/16 heterocycles are of considerable interest in the context of the design and synthesis of advanced functional materials based on radical ions, especially magnetic and conducting materials.[1] Recently, we described the electrochemical and chemical generation of the [1,2,5]thiadiazolo[3,4-*c*][1,2,5]thiadiazolidyl radical anion followed by its isolation in the form of stable salts revealed antiferromagnetic ordering at low temperatures.[2,3] To search new heterocyclic precursors of stable radical ions, we studied the redox properties of 1,3λ⁴δ²,2,4-benzodithiadiazines **1**–**12** in the hydrocarbon and fluorocarbon series (Scheme 1, Table 1). These compounds belong to 12π-electron antiaromatic heterocycles featuring non-trivial heteroatom reactivity.[4–14]

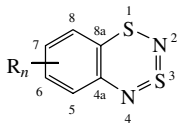

1 R_n = none
2 R_n = 5-Me
3 R_n = 6-Me
4 R_n = 7-Me
5 R_n = 5,7-Bu^t_2
6 R_n = 5-OMe
7 R_n = 6-F
8 R_n = 6,7-F_2
9 R_n = 6,8-F_2
10 R_n = 5,6,7-F_3
11 R_n = 5,6,8-F_3
12 R_n = 5,6,7,8-F_4

Scheme 1

Cyclic voltammograms (CVs)† of **1**–**12** were measured in the $-2.3 < E < 0$ and $0 < E < 2.7$ V potential sweeps for reduction and oxidation, respectively, for solutions in MeCN. Depending upon compound, the CVs revealed one or two reduction peak(s) and two to five oxidation peaks. Since this work is focused on radical ions, only the first steps of both reduction and oxidation of **1**–**12** are discussed below.

For **1**–**12**, both the first oxidation and the first reduction peaks were diffusion-controlled† and related to one-electron

† Compounds **1**–**12** were prepared as described elsewhere.[5,12,14–17] The CV measurements of **1**–**12** were performed at 298 K in an argon atmosphere in absolute MeCN at a stationary platinum electrode with 0.1 M Et_4NClO_4 as a supporting electrolyte with sweep rates of 0.01–100 V s^{-1}. Peak potentials are quoted with reference to a saturated calomel electrode. For **1**–**12**, both the first oxidation and the first reduction peaks are diffusion-controlled, *i.e.*, $I_p^c \nu^{-1/2}$ = const, where I_p is the peak current, and ν is the sweep rate.

Table 1 Experimental redox potentials of **1**–**12** in MeCN,† their gas-phase UB3LYP/6-31G(d) first adiabatic ionization energies (IE_1) and electron affinities (EA_1),‡ and the half-life times ($\tau_{1/2}$) of the radical cations of **1**–**5**,**7** under electrochemical conditions.§

Compound	E_p^{1Red}/V	EA_1/eV	E_p^{1Ox}/V	IE_1/eV	ν^{rev} (≥ V s^{-1})[a]	$\tau_{1/2}$/s at 243 (295) K
1	–0.87[b]	–1.36	1.15	7.11	0.03	~101×10³ (600)
2	–0.90	–1.38	1.11	6.97	0.01	430
3	–0.89	–1.33	1.08	6.97	0.02	105
4	–0.91	–1.33	1.08	6.91	0.02	227
5	–0.95	–1.43	1.01	6.68	0.01	500 (95)
6	–0.88	–1.28	1.07	6.73	0.02	
7	–0.77	–1.56	1.20	7.22	0.3	63
8	–0.75	–1.65	1.23	7.28	0.4	
9	–0.68	–1.67	1.33	7.38	2	
10	–0.67	–1.76	1.33	7.41	1	
11	–0.58	–1.78	1.42	7.50	5	
12	–0.55	–1.86	1.44	7.56	10	

[a]The sweep rate at which a cathode peak in the reverse part of oxidation CV becomes observable. [b]Previously reported –0.57 V.[12] The difference may be due to the different electrodes used: a dropping-mercury electrode[12] and a stationary platinum one (this work).†

‡ The quantum-chemical calculations were performed using the Gaussian 98 suite of programs.[18] The geometries of neutral **1**–**12** and their radical ions were fully optimised at the (U)B3LYP/6-311G(d,p) level of theory. To account for the solvent, the hfc constants in MeCN were calculated at the same level of theory using the polarised continuum model (PCM or Tomasi model)[19] as implemented in the Gaussian 98. The adiabatic IE_1 and EA_1 were calculated as the energy difference between the neutral and corresponding radical ion states. For vertical IEs from HeI UPS, see ref. 11.

§ The ESR spectra were recorded on a Bruker ESP-300 spectrometer (MW power of 265 mW, modulation frequency of 100 KHz and modulation amplitude of 0.005 mT). The generation of radical cations was carried out at 243 K under anaerobic conditions. Simulations of the experimental ESR spectra were performed with the Winsim 32 program (the accuracy in calculating a is ±0.0001 mT).

The half-life times ($\tau_{1/2}$) of radical cations were calculated from the time dependence of the integral intensities of ESR signals in the absence of applied potentials. In the case of **3**–**5**,**7**, those were determined using the first-order rate equation for radical cation decay. For the radical cation of **1**, $\tau_{1/2}$ at 243 K was estimated at the initial stage of decay in a time interval of 3600 s. The experimental kinetic curve of decay of the radical cation of **2** was not of the first order, and $\tau_{1/2}$ is the time at which one half of the initial integral intensity of ESR signal was observed.

Table 2 Experimental hfc constants (mT) of the radical cations of **1**–**7** together with those calculated at the DFT/UB3LYP/6-311G(d,p) level of theory with the PCM model of solvent.‡

	Experimental in MeCN	UB3LYP/6-311G(d,p)	
		Gas phase	MeCN solution
1	0.254 (N2), 0.382 (N4), 0.050 (H5), 0.175 (H6), 0.206 (H7), 0.027 (H8)	0.254 (N2), 0.302 (N4), –0.088 (H5), –0.086 (H6), –0.289 (H7), 0.053 (H8)	0.262 (N2), 0.290 (N4), –0.070 (H5), –0.104 (H6), –0.271 (H7), 0.038 (H8)
2	0.266 (N2), 0.366 (N4), 0.001 (Me), 0.159 (H6), 0.209 (H7), 0.020 (H8)	0.279 (N2), 0.272 (N4), 0.049 (Me), –0.061 (H6), –0.289 (H7), 0.057 (H8)	0.253 (N2), 0.291 (N4), 0.054 (Me), –0.065 (H6), –0.285 (H7), 0.051 (H8)
3	0.222 (N2), 0.377 (N4), 0.003 (H5), 0.248 (Me), 0.227 (H7), 0.227 (H8)	0.220 (N2), 0.303 (N4), –0.050 (H5), 0.086 (Me), –0.343 (H7), 0.068 (H8)	0.198 (N2), 0.318 (N4), –0.061 (H5), 0.164 (Me), –0.325 (H7), 0.058 (H8)
4	0.341 (N2), 0.287 (N4), 0.040 (H5), 0.212 (H6), 0.270 (Me), 0.010 (H8)	0.310 (N2), 0.241 (N4), –0.047 (H5), –0.140 (H6), 0.409 (Me), 0.056 (H8)	0.283 (N2), 0.260 (N4), –0.057 (H5), –0.135 (H6), 0.380 (Me), 0.050 (H8)
5	0.325 (N2), 0.299 (N4), 0.199 (H6), 0.014 (H8)	0.348 (N2), 0.207 (N4), 0.003 (Bu^t), –0.120 (H6), 0.006 (Bu^t), 0.044 (H8)	0.316 (N2), 0.228 (N4), 0.003 (Bu^t), –0.120 (H6), 0.005 (Bu^t), 0.040 (H8)
6	0.342 (N2), 0.328 (N4), 0.047 (OMe), 0.010 (H6), 0.206 (H7), 0.077 (H8)	0.412 (N2), 0.187 (N4), 0.089 (OMe), 0.021 (H6), –0.223 (H7), 0.052 (H8)	0.381 (N2), 0.203 (N4), 0.076 (OMe), 0.014 (H6), –0.231 (H7), 0.050 (H8)
7	0.203 (N2), 0.245 (N4), 0.028 (H5), 0.402 (F6), 0.645 (H7), 0.038 (H8)	0.164 (N2), 0.348 (N4), –0.057 (H5), 0.208 (F6), –0.357 (H7), 0.060 (H8)	0.161 (N2), 0.348 (N4), –0.059 (H5), 0.209 (F6), –0.353 (H7), 0.058 (H8)

transfer. The corresponding cathode and anode peak potentials are presented in Table 1 as E_p^{1Red} and E_p^{1Ox}, respectively; the gas-phase first adiabatic ionization energies (IE_1) and electron affinities (EA_1) from DFT calculations‡ are given for comparison. There is a linear correlation between E_p^{1Red} and E_p^{1Ox} as $E_p^{1Ox} = 1.06E_p^{1Red} + 2.04$ ($r = 0.990$, $s = 0.02$, $n = 12$), and the difference of E_p^{1Red} and E_p^{1Ox} is constant for compounds **1**–**12** (1.99±0.02 V).

The radical anions of **1**–**12** are highly unstable. For **7**–**12**, the first reduction peak is irreversible with all studied sweep rates. For **1**–**6**, the peak is quasi-reversible with the sweep rates of 20–80 V s^{-1} depending upon compound. The stability of radical anions depends on the solvent, and it is higher in DMF than in MeCN. In particular, quasi-reversibility of the first reduction peak of **1** was observed at a sweep rate of 20 V s^{-1} in MeCN, whereas the corresponding sweep rate in DMF was 3 V s^{-1}.

Amongst radical cations of **1**–**12**, those of **1** and its alkyl, alkoxy and monofluoro-substituted derivatives **2**–**7** are long-lived under the CV conditions (Table 1),† whilst the radical cations of higher fluorinated derivatives **8**–**12** are less stable, especially that of **12**.

The radical cations of compounds **1**–**7** were characterised by ESR spectroscopy at 243 K (Figure 1, Table 2)§ and DFT calculations at the UB3LYP/6-311G(d,p) level of theory (Table 2).‡ The calculated hyperfine coupling (hfc) constants agree fairly well with the experimental ones.

It follows from the DFT calculations that the radical cations of **1**–**7** are planar, whereas neutral molecules are bent along the S1···N4 line (Figure 2). This is in accordance with the data of a gas-phase electron diffraction study on **1**[4] (for detailed discussion of molecular conformations, see also refs. 5, 6 and 13). The distortion of radical anions is even more pronounced (Figure 2). For example, the C2–C1–S1–N2 dihedral angle is predicted to be 28.9° for **1** and 44.2° for its radical anion, while the C1–C2–N4–S3 angles of these species are equal to 15.5° and 21.5°, respectively.

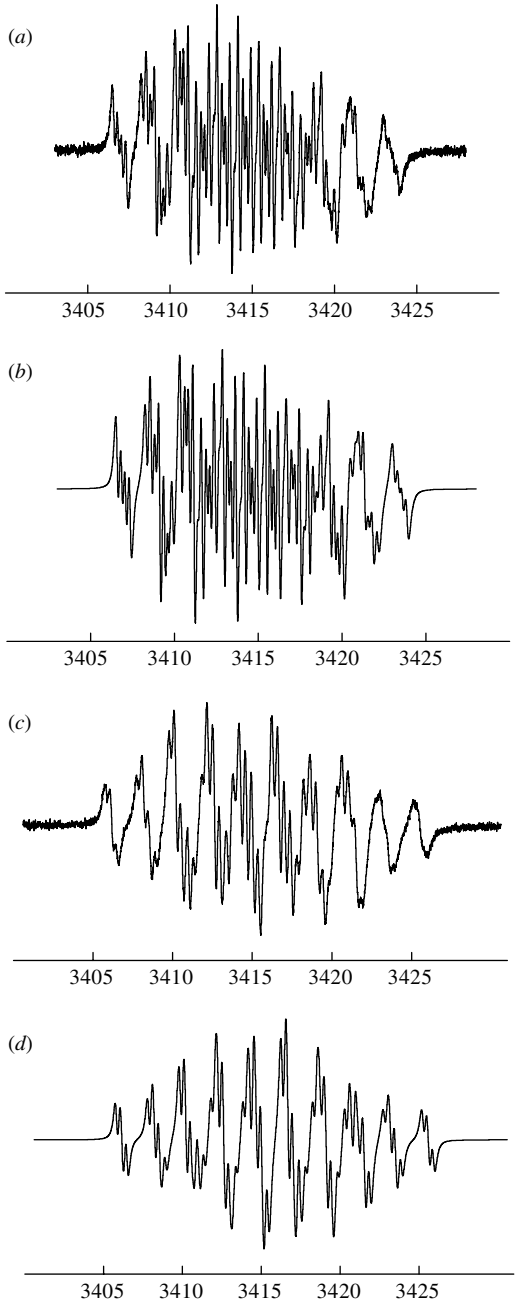

Figure 1 (*a*), (*c*) Experimental and (*b*), (*d*) simulated ESR spectra of radical cations from electrochemical oxidation of (*a*), (*b*) **1** and (*c*), (*d*) **7** at 243 K in MeCN (|H| 10^{-4} T).

Figure 2 displays the most important changes in bond lengths on going from **1** to its radical ions. In the radical anion, the S–N bonds are significantly longer and the C–S and C–N bonds are shorter than that in neutral **1**. This coincides with the structure of the SOMO of the radical anion (Figure 3) featured strong antibonding interaction between S and N atoms and weak bonding interaction between C and S or C and N atoms, respectively. The changes in the geometry of **1** on going to its radical cation could be explained in the same way (Figures 2 and 3).

Figure 3 indicates that the HOMO and LUMO of **1** have similar structures and compositions. These are pseudo π-MOs localised considerably on the heterocycle (atoms S1, N2, S3, N4, C4a, C8a; see Scheme 1). The same is also true for the SOMO of radical ions of **1**. Joint contribution to the frontier MOs of **1**–**12** from the C5–C8 atoms, which bear substituents, is very minor. Due to this, carbocyclic substituents in **1** (Scheme 1,

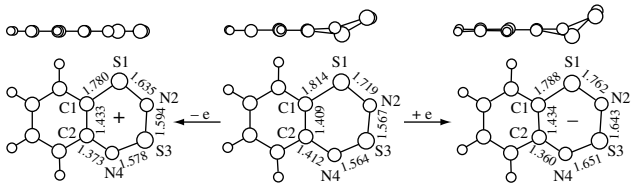

Figure 2 (U)B3LYP/6-311G(d,p) geometry of **1** and its radical ions (bond lengths, Å) (bottom) and their view along the C1–C2 bond (top).

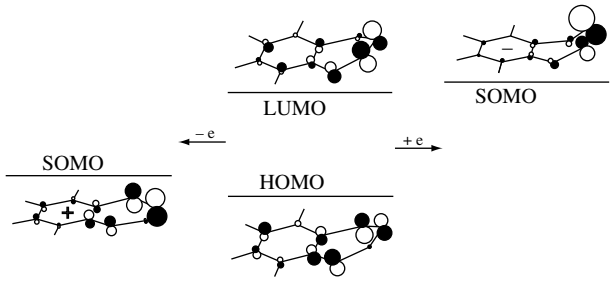

Figure 3 The HOMO and LUMO of **1** and the SOMO of its radical ions calculated by HF and ROHF/6-311G(d,p) methods for (U)B3LYP/6-311G(d,p) geometries.

Table 1) perturb both the HOMO and LUMO only slightly and in a similar way. This leads to the proportional change of the frontier MO energies and the HOMO–LUMO gap remains constant for **1**–**12**. The latter explains the observed correlation between E_p^{1Red} and E_p^{1Ox} in **1**–**12**.

Thus, in contrast to radical anions of the title compounds, their radical cations are relatively stable in the hydrocarbon series under CV conditions.

This work was supported by the Siberian Branch of the Russian Academy of Sciences (interdisciplinary project no. 25) and the Russian Foundation for Basic Research (project no. 04-03-32259). A. Yu. M. and A. V. Z. acknowledge the support of the Council for Grants of the President of the Russian Federation (grant for young scientists and their supervisors no. MK-3178.2005.3); and A. Yu. M. thanks the National Science Support Foundation (Russia) for postdoctoral scholarship. N. P. G. gratefully acknowledges the Ohio Supercomputing Center (USA) for providing computational facilities.

References

1 R. T. Boere and T. L. Roemmele, *Coord. Chem. Rev.*, 2000, **210**, 369.
2 A. Yu. Makarov, I. G. Irtegova, N. V. Vasilieva, I. Yu. Bagryanskaya, T. Borrmann, Yu. V. Gatilov, E. Lork, R. Mews, W.-D. Stohrer and A. V. Zibarev, *Inorg. Chem.*, 2005, **44**, 7194.
3 V. N. Ikorskii, I. G. Irtegova, E. Lork, A. Yu. Makarov, R. Mews, V. I. Ovcharenko and A. V. Zibarev, *Eur. J. Inorg. Chem.*, 2006, 3061.
4 F. Blockhuys, S. L. Hinchley, A. Yu. Makarov, Yu. V. Gatilov, A. V. Zibarev, J. D. Woollins and D. W. H. Rankin, *Chem. Eur. J.*, 2001, **7**, 3592.
5 A. Yu. Makarov, I. Yu. Bagryanskaya, F. Blockhuys, C. Van Alsenoy, Yu. V. Gatilov, V. V. Knyazev, A. Yu. Maksimov, T. V. Mikhalina, V. E. Platonov, M. M. Shakirov and A. V. Zibarev, *Eur. J. Inorg. Chem.*, 2003, 77.
6 A. R. Turner, F. Blockhuys, C. Van Alsenoy, H. E. Robertson, S. L. Hinchley, A. V. Zibarev, A. Yu. Makarov and D. W. H. Rankin, *Eur. J. Inorg. Chem.*, 2005, 572.
7 A. V. Zibarev, Yu. V. Gatilov, I. Yu. Bagryanskaya, A. M. Maksimov and A. O. Miller, *J. Chem. Soc., Chem. Commun.*, 1993, 298.
8 A. Yu. Makarov, I. Yu. Bagryanskaya, Yu. V. Gatilov, M. M. Shakirov and A. V. Zibarev, *Mendeleev Commun.*, 2003, 19.
9 V. V. Zhivonitko, A. Yu. Makarov, I. Yu. Bagryanskaya, Yu. V. Gatilov, M. M. Shakirov and A. V. Zibarev, *Eur. J. Inorg. Chem.*, 2005, 4099.
10 N. P. Gritsan, S. N. Kim, A. Yu. Makarov, E. N. Chesnokov and A. V. Zibarev, *Photochem. Photobiol. Sci.*, 2006, **5**, 95.
11 A. V. Manaev, A. Yu. Makarov, Yu. V. Gatilov, J. N. Latosinska, V. V. Shcherbukhin, V. F. Traven and A. V. Zibarev, *J. Electron Spectrosc. Relat. Phenom.*, 2000, **107**, 33.
12 A. W. Cordes, M. Hojo, H. Koenig, M. C. Noble, R. T. Oakley and W. T. Pennington, *Inorg. Chem.*, 1986, **25**, 1137.
13 K. Tersago, C. De Dobbelaere, C. Van Alsenoy and F. Blockhuys, *Chem. Phys. Lett.*, 2007, **434**, 200.
14 A. V. Zibarev, Yu. V. Gatilov and A. O. Miller, *Polyhedron*, 1992, **11**, 1137.
15 I. Yu. Bagryanskaya, Yu. V. Gatilov, A. Yu. Makarov, A. M. Maksimov, A. O. Miller, M. M. Shakirov and A. V. Zibarev, *Heteroatom Chem.*, 1999, **10**, 113.
16 A. Yu. Makarov, I. Yu. Bagryanskaya, Yu. V. Gatilov, T. V. Mikhalina, M. M. Shakirov, L. N. Shchegoleva and A. V. Zibarev, *Heteroatom Chem.*, 2001, **12**, 563.
17 A. Yu. Makarov, S. N. Kim, N. P. Gritsan, I. Yu. Bagryanskaya, Yu. V. Gatilov and A. V. Zibarev, *Mendeleev Commun.*, 2005, 14.
18 M. J. Frisch, G. W. Trucks, H. B. Schlegel, G. E. Scuseria, M. A. Robb, J. R. Cheeseman, V. G. Zakrzewski, J. A. Montgomery, Jr., R. E. Stratmann, J. C. Burant, S. Dapprich, J. M. Millam, A. D. Daniels, K. N. Kudin, M. C. Strain, O. Farkas, J. Tomasi, V. Barone, M. Cossi, R. Cammi, B. Mennucci, C. Pomelli, C. Adamo, S. Clifford, J. Ochterski, G. A. Petersson, P. Y. Ayala, Q. Cui, K. Morokuma, D. K. Malick, A. D. Rabuck, K. Raghavachari, J. B. Foresman, J. Cioslowski, J. V. Ortiz, B. B. Stefanov, G. Liu, A. Liashenko, P. Piskorz, I. Komaromi, R. Gomperts, R. L. Martin, D. J. Fox, T. Keith, M. A. Al-Laham, C. Y. Peng, A. Nanayakkara, C. Gonzalez, M. Challacombe, P. M. W. Gill, B. Johnson, W. Chen, M. W. Wong, J. L. Andres, C. Gonzalez, M. Head-Gordon, E. S. Replogle and J. A. Pople, *Gaussian 98, Revision A.6*, Gaussian Inc., Pittsburgh, PA, 1998.
19 J. Tomasi, B. Mennucci and R. Cammi, *Chem. Rev.*, 2006, **105**, 2999.

Received: 26th December 2006; Com. 06/2852